DFT-Based Quantitative Prediction of Regioselectivity: Cycloaddition of Nitrilimines to Methyl Propiolate

Alessandro Ponti*,† and Giorgio Molteni‡

Centro per lo Studio delle Relazioni tra Struttura e Reattività Chimica, Consiglio Nazionale delle Ricerche, via Golgi 19, 20133 Milano, Italy, and Dipartimento di Chimica Organica e Industriale, Università degli Studi di Milano, via Golgi 19, 20133 Milano, Italy

ponti@csrsrc.mi.cnr.it

Received March 6, 2001

In the last two decades, many important concepts and indices useful to understand chemical reactivity have been rationalized within the framework of the density functional theory (DFT).[1] Relevant reactivity indices[2] are the electron chemical potential μ, a molecular quantity that measures the escaping tendency of electrons, and the local softness $s(\mathbf{r})$, which represents the sensitivity of the molecular electron density at point $\mathbf{r}$ to a change in μ. Local softness is therefore well suited to compare reactivity at different sites within one molecule. Integration of $s(\mathbf{r})$ over the molecular volume gives the global softness S, which contains information on the reactivity of the molecule as a whole. The link between the DFT indices and chemical reactivity is provided by the hard−soft acid−base principle (HSAB),[3] which also found a convenient theoretical framework within the DFT. This principle is well suited to study chemical reactions since it only requires that temperature is constant and allows for variation in both chemical and external (nuclear) potential. This is at variance with the principle of maximum hardness,[4] which requires that also the chemical and external potentials are constant. The HSAB principle states that when molecule A of softness S_A may react with several partner X of equal chemical potential, it reacts with that partner for which $|S_A - S_X|$ is minimum, i.e., hard likes hard and soft likes soft. The local version[5] of the HSAB principle predicts between which atoms on A and X the new chemical bond forms by using local softness as a reactivity index. Indeed, reliable *qualitative* prediction of regioselectivity has been obtained[6] for several 1,3-dipolar cycloadditions (1,3-DC) by this method.

To predict *quantitative* regioselectivity ratios, one should locate the transition states and compute their energy. This being a difficult task, there is current effort[7] aimed at obtaining activation energies from isolated reactants' properties without locating transition states. In this framework, a generalization of the HSAB principle has been very recently introduced,[8] which enables one to compute, from μ and s of the reactants only, the grand potential[9] variation $\Delta\Omega$ due to the bond-forming interaction between specific atoms of the reactants. Since in 1,3-DCs the relative energy of transition states is paralleled by the relative energy of the weakly interacting complexes forming in the early stage of the reaction,[10] $\Delta\Omega$ is closely related to the transition state energy and can provide a *quantitative* prediction of regioselectivity.

As a first demonstration of this novel method, we turned our attention to nitrilimine 1,3-DCs. These represent a very general route for the construction of a large array of compounds containing the pyrazole ring.[11] Despite the synthetic usefulness of this approach, there is a paucity of data concerning the theoretical aspects of nitrilimine chemistry.[12] For the cycloaddition of nitrilimines to both electron-poor and -rich dipolarophiles, FMO theory predicts full regioselectivity toward the 5-substituted Δ^2-pyrazolines.[10] This prediction is obeyed in the vast majority of 1,3-DCs of nitrilimines to monosubstituted ethenes.[11b,c] Conversely, addition of diphenylnitrilimine to methyl propiolate yields a mixture of regioisomeric 5- and 4-pyrazolines in 78:22 ratio.[13] We were thus prompted to investigate the regiochemistry of the 1,3-DC between a series of *C*-carbomethoxy-*N*-(4-substituted)phenyl nitrilimines **2** to methyl propiolate **3** (see Scheme 1). In particular, we show how the DFT/HSAB approach corrects this FMO theory prediction, and we demonstrate the validity of the novel quantitative

* To whom correspondence should be addressed. Fax (+39)-0270638129.

† Consiglio Nazionale delle Ricerche.

‡ Università degli Studi di Milano.

(1) Parr, R. G.; Yang, W. *Density Functional Theory of Atoms and Molecules*; Oxford University Press: Oxford, 1989.

(2) Chermette, H. *J. Comput. Chem.* **1999**, *20*, 129−154.

(3) (a) Pearson, R. G. *J. Am. Chem. Soc.* **1963**, *85*, 3533−3539. (b) Chattaraj, P. K.; Lee, H.; Parr, R. G. *J. Am. Chem. Soc.* **1991**, *113*, 1855−1856. (c) Cedillo, A.; Chattaraj, P. K.; Parr, R. G. *Int. J. Quantum Chem.* **2000**, *77*, 403−407.

(4) Parr, R. G.; Chattaraj, P. K. *J. Am. Chem. Soc.* **1991**, *113*, 1854−1855.

(5) Gázquez, J. L.; Méndez, F. *J. Phys. Chem.* **1994**, *98*, 4591−4593.

(6) (a) Chandra, A. K.; Nguyen, M. T. *J. Comput. Chem.* **1998**, *19*, 195−202. (b) Chandra, A. K.; Nguyen, M. T. *J. Phys. Chem. A* **1998**, *102*, 6181−6185. (c) Mendez, F.; Tamariz, J.; Geerlings, P. *J. Phys. Chem. A* **1998**, *102*, 6292−6296. (d) Le, T. N.; Nguyen, L. T.; Chandra, A. K.; De Proft, F.; Geerlings, P.; Nguyen, M. T. *J. Chem. Soc., Perkin Trans. 2* **1999**, 1249−1255. (e) Chandra, A. K.; Uchimaru, T.; Nguyen, M. T. *J. Chem. Soc., Perkin Trans. 2* **1999**, 2117−2121.

(7) (a) Gázquez, J. L. *J. Phys. Chem.* **1997**, *101*, 8967−8969. (b) Toro-Labbè, A. *J. Phys. Chem.* **1999**, *103*, 4398−4403. (c) Clark, L. A.; Ellis, D. E.; Snurr, R. Q. *J. Chem. Phys.* **2001**, *114*, 2580−2591.

(8) Ponti, A. *J. Phys. Chem. A* **2000**, *104*, 8843−8846.

(9) The grand potential $\Omega = E - N\mu$, where E is energy, N is the number of electrons, and μ is the electron chemical potential, is the natural thermodynamic quantity to describe the behavior of the reactants' atoms, which are open subsystems freely exchanging energy and electrons.

(10) Houk, K. N.; Sims, J.; Watts, C. R.; Luskus, L. J. *J. Am. Chem. Soc.* **1973**, *95*, 7301−7315.

(11) (a) Caramella, P.; Grünanger, P. In *1,3-Dipolar Cycloaddition Chemistry*; Padwa, A., Ed.; John Wiley & Sons: New York, 1984; Vol. 1, Chapter 3, pp 291−392. (b) Claus, P. K. In *Methoden der Organischen Chemie* (*Houben-Weil*); Klaman, D., Hageman, H., Eds.; Georg Thieme Verlag: Stuttgart, 1990; Band E14b, Teil 1, pp 33−73. (c) Shawali, A. S.; Pàrkàni, C. *J. Heterocycl. Chem.* **1980**, *17*, 833−854. (d) Bianchi, G.; De Micheli, C.; Gandolfi, R. In *The Chemistry of Double Bonded Functional Groups*; Patai, S., Ed.; Wiley: London, 1977; Part I, Chapter 6, pp 369−532. (e) Padwa, A. In *Comprehensive Organic Synthesis*; Trost, B., Ed.; Pergamon Press: New York, 1992; Vol. 4, Chapter 4/9, pp 1069−1109. (f) Wade, P. A. In *Comprehensive Organic Synthesis*, Trost B. Ed.; Pergamon Press: New York, 1992; Vol. 4, Chapter 4/10, pp 1110−1168. (g) Bertrand, G.; Wentrup, C. *Angew. Chem., Int. Ed.* **1994**, **33**, 527−545. (h) Molteni, G.; Zecchi, G. *Trends Heterocyclic Chem.* **1997**, *5*, 127−133. (i) Broggini, G.; Molteni, G.; Zecchi, G. *Heterocycles* **1998**, *47*, 541−557. (j) Broggini, G.; Garanti, L.; Molteni, G.; Pilati, T.; Ponti, A.; Zecchi, G. *Tetrahedron*: *Asymmetry* **1999**, *10*, 2203−2212. (k) Broggini, G.; Molteni, G. *J. Chem. Soc., Perkin Trans. 1* **2000**, 1685−1689.

(12) (a) Reference 11a. (b) Caramella, P.; Houk, K. N. *J. Am. Chem. Soc.* **1976**, *98*, 6397−6399. (c) Krajsovszky, G.; Gaal, A.; Haider, N.; Matyus, P. *Theochem-J. Mol. Struct.* **2000**, *528*, 13−18.

(13) Huisgen, R.; Sustmann, R.; Wallbillich, G. *Chem. Ber.* **1967**, *100*, 1786−1801.

10.1021/jo0156159 CCC: $20.00
Published on Web 06/28/2001

Scheme 1. Cycloaddition of Nitrilimines 2 with Propiolate 3.

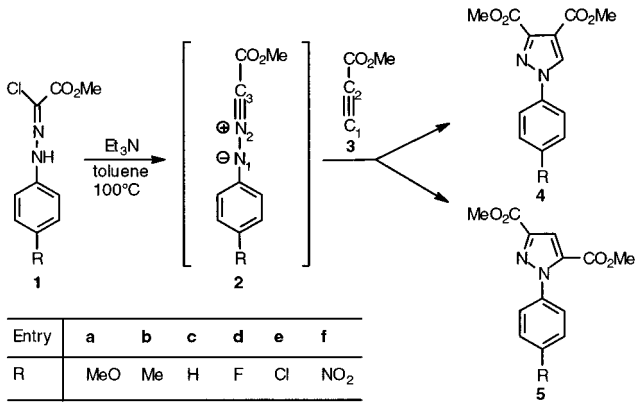

Entry	a	b	c	d	e	f
R	MeO	Me	H	F	Cl	NO_2

Table 1. Experimental Reaction Times and Yields and 4:5 Yield Ratio of the Cycloaddition between Nitrilimines 2 and Methyl Propiolate 3

entry	time (min)	yields[a] (%) 1	yields[a] (%) 4 + 5	yield ratio[b] 4:5
a	20	6	63	56:44
b	30	0	95	66:34
c	45	8	69	56:44
d	60	11	48	53:47
e	60	10	50	52:48
f	240	0	6	51:49

[a] Isolation yields. [b] Deduced from ^{1}H NMR of reaction crudes.

method by comparing the regioisomeric ratio obtained from experiment to that computed from DFT reactivity indices via the generalized HSAB principle and finding very good agreement.

Labile intermediates **2** were generated in situ by base treatment of the corresponding hydrazonoyl chlorides **1**[14] according to a well-established procedure.[13] Subsequent reaction with **3** gave the isomeric adducts **4** and **5,** and their structure was firmly established by ^{1}H NMR, since protons in the 4- and 5- positions of the pyrazolic ring show resonances in perfect agreement with literature values.[15] Reaction times and yields are reported in Table 1. Despite the modest regioselectivity, the favored product clearly is the 4-substituted regioisomer.

The main results of DFT calculations at the B3LYP/6-311+G(*d*,*p*) level are reported in Table 2. The electron chemical potential difference between **2** and **3** determines the direction of the overall charge flow upon interaction of the reactants, as electrons flow toward regions at low μ. It turns out that **2a**-**e** act as nucleophiles whereas **2f** acts as electrophile (note, however, that the chemical potentials of **2f** and of **3** are very close to each other). Notwithstanding that our calculations show that reactions of **3** with **2a**−**e** are HOMO-dipole controlled in agreement with FMO theory, the latter predicts that nitrilimines **5a**−**e** are the favored regioisomers, in contrast with experiment. As for the reaction of **3** with the electron-poor nitrilimine **2f**, FMO theory is not able to provide a clear-cut prediction since the two HOMO−LUMO interactions are comparable in size.

Table 2. Results of B3LYP/6-311+G(*d*,*p*) Calculations. Chemical Potential Difference between Nitrilimines 2 and Methyl Propiolate 3 and ΔΔΩ Difference[a] and Predicted 4:5 Yield Ratio for Their Mutual Cycloaddition

entry	μ(**2**) − μ(**3**) (eV)	$\delta\Delta\Omega$ (kJ mol^{-1})	predicted ratio[b] **4**:**5n**
a	1.85	−0.64	56:44
b	2.17	−1.70	66:34
c	1.57	−0.34	54:46
d	1.43	−0.34	54:46
e	1.35	−0.39	54:46
f	−0.08	-0.49×10^{-4}	51:49

[a] Difference in grand potential variation for the pathways leading to products **4** and **5**. [b] From computed $\delta\Delta\Omega$ and eq 3; uncertainty ±1%.

From the electron chemical potential μ and the local softness s (condensed to individual atoms), one can compute the charge transfers between interacting atom pairs.[5] For instance, the charge transfer from N_1 of **2** to C_1 of **3** amounts to (see Scheme 1 for numbering)

$$\Delta q(N_1 \rightarrow C_1) = -[\mu(\mathbf{2}) - \mu(\mathbf{3})]\, s(N_1)\, s(C_1)\, [s(N_1) + s(C_1)]^{-1} \quad (1)$$

It is noteworthy that, except for **2f**, the atom−atom charge transfers mimic the usual arrow notation. C_1 (C_2) accepts (donates) electrons irrespective of the resulting cycloadduct. Conversely, N_1 (C_3) accepts (donates) electrons when isomer **5** is formed but the reverse occurs when the product is **4**. However, local softness is most important in the context of regioselectivity prediction. As selectivity criterion,[8] we used the grand potential change due to *two* bond-forming interactions between **2** and **3**, because of the general agreement about the concertedness of 1,3-DC reactions.[10] The grand potential change for the pathway leading to isomer **4** is

$$\Delta\Omega(\mathbf{4}) = -(1/2)\, [\mu(\mathbf{2}) - \mu(\mathbf{3})]^2 \{s(N_1)\, s(C_1)\, [s(N_1) + s(C_1)]^{-1} + s(C_3)\, s(C_2)\, [s(C_3) + s(C_2)]^{-1}\} \quad (2)$$

$\Delta\Omega$(**5**) can be obtained by exchanging $s(C_1)$ and $s(C_2)$. The difference $\delta\Delta\Omega = \Delta\Omega(\mathbf{4}) - \Delta\Omega(\mathbf{5})$ is reported in Table 2.

As stated previously, one expects that $\delta\Delta\Omega$ accounts for most of the energy difference between the transition states leading to **4** and **5**. The negative sign of $\delta\Delta\Omega$ shows that, in the considered 1,3-DCs, isomer **4** is the major one, in line with the experimental results but in contrast to FMO theory. We now proceed one step further by demonstrating that $\delta\Delta\Omega$ is a quantitative regioselectivity index for 1,3-DC reactions. The difference in activation energy $\delta\Delta$E of the two reaction paths can be obtained as $\delta\Delta E = -RT \log(Y)$, where $T = 373$ K is the reaction temperature and Y is the experimental **4**:**5** ratio. Estimating the error in Y at ±1%, weighted least-squares linear regression results in

$$\delta\Delta\Omega = (1.15 \pm 0.07)\, \delta\Delta E - (0.06 \pm 0.05) \quad (3)$$

with correlation coefficient $\rho = 0.956$ (see Figure 1). The statistically insignificant intercept shows that $\delta\Delta\Omega$ is truly proportional to the difference in transition-state energy. The predicted **4**:**5** ratios (Table 2), obtained from

(14) (a) **1a**,**b**,**e**: Cusumano, G.; Macaluso, G.; Hinz, W.; Buscemi, S. *Heterocycles* **1987**, *26*, 1283−1289. (b) **1c**: El-Abadelah, M. M.; Hussein, A. Q.; Kamal, M. R.; Al-Ashami, K H. *Heterocycles* **1988**, *27*, 917−924. (c) **1d**,**f**: El-Abadelah, M. M.; Hussein, A. Q.; Saadeh, H. A *Heterocycles* **1991**, *32*, 1063−1079.

(15) (a) Batterham, T. J. *NMR Spectra of Simple Heterocycles*; Wiley: New York, 1973. (b) Katritzky, A. R.; Lagowski, J. M. In *Comprehensive Heterocyclic Chemistry*; Katritzky, A. R., Rees, C. W., Eds.; Pergamon Press: Oxford, 1985; Vol. 5, Chapter 4.01, pp 2−38.

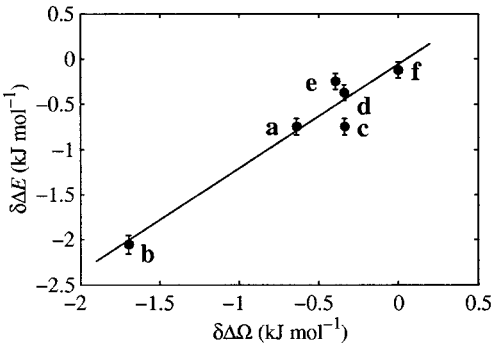

Figure 1. Linear relationship between the computed difference $\delta\Delta\Omega$ in grand potential variation for the pathways leading to products **4** and **5** and the correspondent difference in activation energy $\delta\Delta E$, computed from the experimental ratio. The error bars show the uncertainty in $\delta\Delta E$ due to the error in the **4**:**5** ratio, estimated at 1%.

computed $\delta\Delta\Omega$ via eq 3, are in good agreement with the experimental values (Table 1).

The very low selectivity of the reaction of **2f** with **3** is due to two concurrent causes. First, μ(**2f**) and μ(**3**) are so close that $\Delta\Omega$ (and hence $\delta\Delta\Omega$) is nearly 3 orders of magnitude smaller than in the remaining cases. Besides, the grand potential change due to the formation of the N_1-C_1 bond is close to that for the N_1-C_2 bond; the same occurs for the C_3-C_1 and the C_3-C_2 bonds. At the other extreme, **2b** shows higher selectivity toward **4b**, a fact somewhat unexpected on the basis of the usual substituent effect. Indeed, **2b** has the highest chemical potential (see Table 2) but this fact alone is not sufficient to account for the large difference in $\Delta\Omega$. Dissecting the latter into bond contributions, it turns out that the high selectivity is caused by the particularly unfavorable interaction between N_1 and C_2.

We have thus shown that the combined use of DFT reactivity indices (of the reactants) with the HSAB principle is superior to FMO theory in predicting the favored regioisomer, and most important, it provides quantitative prediction of regioselectivity and insight into the details of atom−atom interactions in 1,3-DC reactions without the need of locating transition states or even characterizing products.

Experimental Section

Computational Methods. DFT calculations were performed by means of the GAUSSIAN 94 program suite.[16] The hybrid B3LYP functional was employed with the standard 6-311+G(*d*,*p*) basis set. Geometry of **2a**−**f** and **3** was fully optimized and characterized with vibrational analysis at the same level of theory. The anion and cation of **2a**−**f** and **3** were treated at the UB3LYP/6-311+G(*d*,*p*) level using the geometry of the neutral systems. Atomic electron populations were evaluated following the Merz−Kollman scheme.[17] This scheme, which already proved to be reliable,[18] has been used in most DFT calculations of regiochemistry of 1,3-DCs,[6] so that our results can be directly compared with existing literature. It has also been recently considered as an appropriate local descriptor of charge.[19] Reactivity indices were computed within the finite difference approximation:[1] $\mu = -(\mathrm{IP} + \mathrm{EA})/2$ and $S = (\mathrm{IP} - \mathrm{EA})^{-1}$, where IP and EA are the (vertical) ionization potential and electron affinity, respectively. The local softness s (condensed to each individual atom[20]) was computed as $s = S\,[p(N_0 + 1) - p(N_0)]$ for electrophiles, and as $s = S\,[p(N_0) - p(N_0 - 1)]$ for nucleophiles, where $p(N)$, $N = N_0 - 1$, N_0, $N_0 + 1$, is the atomic electron population of the cationic, neutral, and anionic system, respectively.

General Methods. Melting points were determined in open tubes and are uncorrected. IR spectra were recorded with a FT-IR spectrophotometer. Mass spectra were determined with a 70 eV EI apparatus. ^{1}H NMR (300 MHz), ^{13}C NMR (75 MHz), and ^{19}F NMR (282 MHz) spectra were taken in $CDCl_3$ solutions at 297 K. Chemical shifts are given as ppm from tetramethylsilane (hexafluorobenzene for ^{19}F NMR); J values are given in Hz.

Cycloaddition between Nitrilimines 2 and Methyl Propiolate 3: General Procedure. A solution of **1** (2.0 mmol) and **3** (0.34 g, 4.0 mmol) in dry toluene (20 mL) was added with triethylamine (1.01 g, 10 mmol) and then heated to 100 °C for the time indicated in Table 1. Evaporation of the solvent in vacuo gave a residue which was chromatographed on a silica gel column with ethyl acetate−hexane 1:1. Unreacted **1** was eluted first, followed by the pyrazolic cycloadduct **4**; further elution gave **5**. Crystallization from diisopropyl ether gave analytically pure **4** and **5**.

4a: 0.16 g, 28%; pale yellow solid; mp 103−105 °C; ^{1}H NMR (300 MHz, $CDCl_3$): δ 3.83 (3H, s), 3.90 (3H, s), 3.95 (3H, s), 7.48 (1H, s), 7.10−7.30 (4H, m); ^{13}C NMR (75 MHz, $CDCl_3$) δ 44.12 (q), 52.13 (q), 53.50 (q), 120.0−127.0, 128.20 (d), 135.21 (s), 137.26 (s), 144.13 (s), 158.66 (s), 161.21 (s), 162 0.10 (s); IR (Nujol) 1730 cm^{-1}; MS *m*/*z* 290 (M^+). Anal. Calcd for $C_{14}H_{14}N_2O_5$: C, 57.93; H, 4.86; N, 9.65. Found: C, 57.87; H, 4.80; N, 9.62.

4b: 0.18 g, 32%; white solid; mp 96−97 °C; ^{1}H NMR (300 MHz, $CDCl_3$) δ 2.42 (3H, s), 3.81 (3H, s), 3.96 (3H, s), 7.20−7.30 (4H, m), 7.50 (1H, s); ^{13}C NMR (75 MHz, $CDCl_3$) δ 20.82 (q), 52.60 (q), 52.88 (q), 120.0−125.4, 128.16 (d), 135.02 (s), 136.60 (s), 142.10 (s), 158.95 (s), 161.55 (s), 162 0.90 (s); IR (Nujol) 1725 cm^{-1}; MS *m*/*z* 274 (M^+). Anal. Calcd for $C_{14}H_{14}N_2O_3$: C, 61.31; H, 5.14; N, 10.21. Found: C, 61.23; H, 5.17; N, 10.24.

4c: 0.16 g, 30%; white solid; mp 100−102 °C; ^{1}H NMR (300 MHz, $CDCl_3$) δ 3.81 (3H, s), 3.94 (3H, s), 7.40−7.46 (5H, m), 7.51 (1H, s); ^{13}C NMR (75 MHz, $CDCl_3$) δ 52.21 (q), 52.0 (q), 114.0−128.0, 128.99 (d), 134.31 (s), 139.65 (s), 143.27 (s), 158.76 (s), 161.90 (s); IR (Nujol) 1720 cm^{-1}; MS *m*/*z* 260 (M^+). Anal. Calcd for $C_{13}H_{12}N_2O_4$: C, 60.00; H, 4.65; N, 10.76. Found: C, 59.98; H, 4.60; N, 10.71.

4d: 0.13 g, 23%; pale yellow solid; mp 73−74 °C; ^{1}H NMR (300 MHz, $CDCl_3$) δ 3.81 (3H, s), 3.95 (3H, s), 7.25−7.40 (4H, m), 7.53 (1H, s); ^{13}C NMR (75 MHz, $CDCl_3$) δ 52.67 (q), 52.75 (q), 118.0−125.0, 127.98 (d), 133.72 (s), 135.80 (s), 159.95 (s), 160.80 (s), 162.06 (s); ^{19}F NMR (282 MHz, $CDCl_3$) δ −96.42; IR (Nujol) 1735 cm^{-1}; MS *m*/*z* 278 (M^+). Anal. Calcd for $C_{13}H_{11}FN_2O_4$: C, 56.12; H, 3.98; N, 10.07. Found: C, 56.15; H, 4.04; N, 10.11.

4e: 0.15 g, 26%; pale yellow solid; mp 102−103 °C; ^{1}H NMR (300 MHz, $CDCl_3$) δ 3.80 (3H, s), 3.96 (3H, s), 7.25−7.32 (4H, m), 7.46 (1H, s); ^{13}C NMR (75 MHz, $CDCl_3$) δ 51.90 (q), 53.22 (q), 116.0−124.8, 128.90 (d), 135.23 (s), 138.39 (s), 153.12 (s), 161.22 (s), 164.13 (s); IR (Nujol) 1730 cm^{-1}; MS *m*/*z* 295 (M^+). Anal. Calcd for $C_{13}H_{11}ClN_2O_4$: C, 52.98; H, 3.76; N, 9.51. Found: C, 52.92; H, 3.73; N, 9.57.

4f: 18 mg, 3%; yellow solid; mp 114−116 °C; ^{1}H NMR (300 MHz, $CDCl_3$) δ 3.76 (3H, s), 3.96 (3H, s), 7.59 (1H, s), 7.75−8.20 (4H, m); ^{13}C NMR (75 MHz, $CDCl_3$) δ 52.28 (q), 54.11 (q), 122.1−126.7, 129.90 (d), 139.10 (s), 154.43 (s), 160.02 (s), 161.97 (s), 165.53 (s); IR (Nujol) 1740 cm^{-1}; MS *m*/*z* 305 (M^+). Anal. Calcd for $C_{13}H_{11}N_3O_6$: C, 51.15; H, 3.63; N, 13.77. Found: C, 51.18; H, 3.69; N, 13.70.

(16) Frisch, M. J.; Trucks, G. W.; Schlegel, H. B.; Gill, P. M. W.; Johnson, B. G.; Robb, M. A.; Cheeseman, J. R.; Keith, T.; Petersson, G. A.; Montgomery, J. A.; Raghavachari, K.; Al-Laham, M. A.; Zakrzewski, V. G.; Ortiz, J. V.; Foresman, J. B.; Cioslowski, J.; Stefanov, B. B.; Nanayakkara, A.; Challacombe, M.; Peng, C. Y.; Ayala, P. Y.; Chen, W.; Wong, M. W.; Andres, J. L.; Replogle, E. S.; Gomperts, R.; Martin, R. L.; Fox, D. J.; Binkley, J. S.; Defrees, D. J.; Baker, J.; Stewart, J. P.; Head-Gordon, M.; Gonzalez, C.; Pople, J. A. *Gaussian 94*; Revision E.1; Gaussian, Inc.: Pittsburgh, PA, 1995.

(17) (a) Singh, U. C.; Kollman, P. A. *J. Comput. Chem.* **1984**, *5*, 129−145. (b) Besler, B. H.; Merz, K. M., Jr.; Kollman, P. A. *J. Comput. Chem.* **1990**, *11*, 431−439.

(18) De Proft, F.; Martin, J. M. L.; Geerlings, P. *Chem. Phys. Lett.* **1996**, *250*, 393−401.

(19) Chattaraj, P. K. *J. Phys. Chem.* **2001**, *105*, 511−513.

(20) Yang, W.; Mortier, W. J. *J. Am. Chem. Soc.* **1986**, *108*, 5708−5711.

5a: 0.20 g, 35%; pale yellow solid; mp 94−95 °C; ^{1}H NMR (300 MHz, $CDCl_3$) δ 3.84 (3H, s), 3.89 (3H, s), 3.93 (3H, s), 7.08 (1H, s), 7.10−7.30 (4H, m). ^{13}C NMR (75 MHz, $CDCl_3$) δ 46.36 (q), 53.16 (q), 53.25 (q), 116.14 (d), 118.5−129.0, 137.18 (s), 139.46 (s), 159.54 (s), 162.18 (s); IR (Nujol) 1730, 1720 cm^{-1}; MS *m*/*z* 290 (M^+). Anal. Calcd for $C_{14}H_{14}N_2O_5$: C, 57.93; H, 4.86; N, 9.65. Found: C, 57.89; H, 4.81; N, 9.71.

5b: 0.34 g, 63%; white solid; mp 92 °C; ^{1}H NMR (300 MHz, $CDCl_3$) δ 2.41 (3H, s), 3.81 (3H, s), 3.95 (3H, s), 7.15 (1H, s), 7.20−7.30 (4H, m); ^{13}C NMR (75 MHz, $CDCl_3$) δ 20.97 (q), 52.62 (q), 53.25 (q), 114.54 (d), 120.0−129.0, 138.16 (s), 143.27 (s), 158.84 (s), 161.93 (s); IR (Nujol) 1730, 1720 cm^{-1}; MS *m*/*z* 274 (M^+). Anal. Calcd for $C_{14}H_{14}N_2O_3$: C, 61.31; H, 5.14; N, 10.21. Found: C, 61.25; H, 5.11; N, 10.15.

5c: 0.20 g, 39%; white solid; mp 90−92 °C; ^{1}H NMR (300 MHz, $CDCl_3$) δ 3.81 (3H, s), 3.94 (3H, s), 7.25 (1H, s), 7.40−7.48 (5H, m); ^{13}C NMR (75 MHz, $CDCl_3$): δ 52.19 (q), 52.91 (q), 118.27 (d), 114.0−128.0, 134.42 (s), 139.51 (s), 143.34 (s), 155.75 (s), 161.77 (s); IR (Nujol) 1730, 1720 cm^{-1}; MS *m*/*z* 260 (M^+). Anal. Calcd for $C_{13}H_{12}N_2O_4$: C, 60.00; H, 4.65; N, 10.76. Found: C, 59.93; H, 4.62; N, 10.69.

5d: 0.14 g, 25%; pale yellow solid; mp 70−71 °C; ^{1}H NMR (300 MHz, $CDCl_3$) δ 3.80 (3H, s), 3.96 (3H, s), 7.08 (1H, s), 7.25−7.40 (4H, m); ^{13}C NMR (75 MHz, $CDCl_3$) δ 52.11 (q), 52.40 (q), 115.17 (d), 119.0−130.0, 135.16 (s), 136.44 (s), 155.75 (s), 159.90 (s), 161.77 (s); ^{19}F NMR (282 MHz, $CDCl_3$) δ −101.80; IR (Nujol) 1730, 1720 cm^{-1}; MS *m*/*z* 278 (M^+). Anal. Calcd for $C_{13}H_{11}FN_2O_4$: C, 56.12; H, 3.98; N, 10.07. Found: C, 56.05; H, 4.02; N, 10.15.

5e: 0.14 g, 24%; pale yellow solid; mp 95−96 °C; ^{1}H NMR (300 MHz, $CDCl_3$) δ 3.80 (3H, s), 3.95 (3H, s), 7.20 (1H, s), 7.25−7.32 (4H, m); ^{13}C NMR (75 MHz, $CDCl_3$) δ 52.30 (q), 52.39 (q), 118.05 (d), 120.0−133.0, 134.11 (s), 137.33 (s), 157.76 (s), 160.79 (s), 162.24 (s); IR (Nujol) 1735, 1730 cm^{-1}; MS *m*/*z* 295 (M^+). Anal. Calcd for $C_{13}H_{11}ClN_2O_4$: C, 52.98; H, 3.76; N, 9.51. Found: C, 53.05; H, 3.80; N, 9.49.

5f: 19 mg, 3%; yellow solid; mp 105 °C; ^{1}H NMR (300 MHz, $CDCl_3$) δ 3.82 (3H, s), 3.96 (3H, s), 7.24 (1H, s), 7.75−8.20 (4H, m); ^{13}C NMR (75 MHz, $CDCl_3$) δ 51.56 (q), 52.96 (q), 118.12 (d), 123.0−135.0, 139.30 (s), 160.19 (s), 162.87 (s), 166.80 (s); IR (Nujol) 1740, 1730 cm^{-1}; MS *m*/*z* 305 (M^+). Anal. Calcd for $C_{13}H_{11}N_3O_6$: C, 51.15; H, 3.63; N, 13.77. Found: C, 51.11; H, 3.59; N, 13.82.

Supporting Information Available: Geometry, energy, ionization potential, electron affinity, electron chemical potential, and global softness of **2** and **3**. Merz−Kolmann atomic charge, local softness, and charge transfer of selected atoms of **2** and **3**. This material is available free of charge via the Internet at http://pubs.acs.org.

JO0156159